International Communications in Heat and Mass Transfer 57 (2014) 208–215

Contents lists available at ScienceDirect

International Communications in Heat and Mass Transfer

journal homepage: www.elsevier.com/locate/ichmt

Comparative study on heat transfer characteristics of sintered and mesh wick heat pipes using CuO nanofluids☆

G. Kumaresan [a,*], S. Venkatachalapathy [a], Lazarus Godson Asirvatham [b], Somchai Wongwises [c]

[a] Department of Mechanical Engineering, National Institute of Technology, Tiruchirappalli 620015, Tamil Nadu, India
[b] Department of Mechanical Engineering, Karunya University, Coimbatore 641 114, Tamil Nadu, India
[c] Fluid Mechanics, Thermal Engineering and Multiphase Flow Research Lab (FUTURE), Department of Mechanical Engineering, Faculty of Engineering, King Mongkut's University of Technology, Thonburi, 126 Bangmod, Tongkru, Bangkok 10140, Thailand

ARTICLE INFO

Available online 10 August 2014

Keywords:
Heat pipe
Nanofluid
Wick structure
Surface temperature
Thermal conductivity

ABSTRACT

An experimental investigation has been carried out to compare the enhancement in the thermal performance of sintered and mesh wick heat pipes by varying the working fluid, inclination angle and heat input. Similar geometrical specifications of 12, 330 and 1 mm respectively are selected for the outer diameter, length and wick thickness and kept constant for both sintered and mesh wick heat pipes. The study focuses on changes in surface temperature distribution, thermal resistance and effective thermal conductivity of heat pipes. The results showed that the maximum reduction in surface temperature is obtained for sintered wick heat pipe at 45° tilt angle and 60° for mesh wick heat pipe with CuO/DI water nanofluid concentration at 1.0 wt.% for both the cases. The reduction in thermal resistance of sintered wick heat pipe is 13.92% higher compared with mesh wick heat pipe for the same heat input, mass concentration and inclination angle. Presence of CuO nanoparticles in DI water and increasing heat input tremendously increases the thermal conductivity of heat pipes. An important observation from this study is the sole effect of sintered wick in heat pipe not only reduces the thermal resistance but also increases the heat transport capacity up to 20 W compared with that of mesh wick.

1. Introduction

Phase change heat transfer is suitable for transferring large amount of heat compared with single-phase convective heat transfer. This is because the heat transfer coefficient associated with the boiling and condensation processes are high. Heat pipe is one of such a passive device, which works on the principle of phase change heat transfer. The contribution of heat pipe to the engineering field is remarkable and some of the applications are electronics cooling [1,2], solar heaters [3], air conditioning [4] and HVAC system [5]. Particularly, electronic field is the fast developing one and the heat dissipation in electronic devices is the major problem up-to-date. The performance of heat pipe is limited to the thermal properties of working fluid. Recently, the nanofluids are used to improve the performance of heat pipes instead of conventional fluid. Various authors reported the use of nanofluids instead of base fluids led to a massive reduction in heat pipe thermal resistance [6–8] and wall temperature [6,8,10], meanwhile increase in the thermal conductivity [9,11,12] of heat pipe. Hussein et al. [13] conducted an elaborative review on the heat transfer enhancement and hydrodynamic characteristics of nanofluids. They concluded that the thermal properties of solid nanoparticles enhance the hydrodynamic and heat transfer characteristics of the base fluid. Bahiraei [14] presented an overview on different numerical approaches for simulation in nanofluids. The authors suggested that the use of two phase approach would give better understanding of nanofluids than single phase approach. Loh et al. [15] conducted a study on heat pipes with different wick structures viz. mesh, grooved and sintered metal powder. The test was conducted with increasing power input and the heat pipe orientation was varied from −90° to +90°. They concluded that the sintered powder metal wick structure performance was better compared with mesh and grooved wicks. This is due to the good capillary action in sintered wicks. Putra et al. [16] tested the thermal performance of screen mesh wick heat pipe using Al_2O_3, TiO_2 and ZnO nanoparticles in DI water and ethylene glycol base fluids. They observed a decreasing trend in the temperature difference of the heat pipes with increasing concentrations of Al_2O_3 nanofluids.

Tsai et al. [17] investigated the thermal performance of circular mesh wick heat pipe with Au/DI water nanofluid. The authors reported a reduction in thermal resistance with gold nanofluid compared with DI water. Kempers et al. [18] conducted an experimental study in mesh wick heat pipes by varying the number of wick layers, 1, 2, 3 and 6. They found that the performance of heat pipe was maximum with three layers of mesh wick and observed the lowest thermal resistance. Kumaresan et al. [19] experimentally investigated the thermal

☆ Communicated by W.J. Minkowycz.

* Corresponding author.
E-mail addresses: kumareshgct@gmail.com, 411111053@nitt.edu (G. Kumaresan).

http://dx.doi.org/10.1016/j.icheatmasstransfer.2014.08.001
0735-1933/

Nomenclature

A	surface area (m^2)
D	outer diameter (mm)
d	particle size (nm)
I	current (A)
k	thermal conductivity (W/m°C)
L	length (mm)
Q	heat supplied (W)
R	thermal resistance (°C/W)
T	temperature (°C)
V	voltage (V)
ΔT	temperature difference (°C)

Subscripts

c	condenser
c/s	cross-sectional
e	evaporator
hp	heat pipe
s	surface

Greek symbols

θ	inclination angle (°)
μ	dynamic viscosity (cP)
ω	weight fraction (wt.%)
Δ	increment

characteristics of copper sintered wick heat pipe with CuO/DI water nanofluids. The authors compared the surface and vapor temperatures of heat pipe and they observed a difference of 5.1 °C at the evaporator section. Kang et al. [20] experimentally investigated the thermal performance of sintered wick heat pipes with 10 and 35 nm size silver nanoparticles. It was found that the addition of nanoparticles considerably reduced the temperature difference between the evaporator and condenser ends and enhanced the heat transfer capacity of heat pipe up to 28.6% compared with DI water. Liu and Zhu [21] studied the performance of horizontal mesh wick heat pipe with different concentrations of CuO/DI water nanofluids at subatmospheric pressures. An optimum concentration of CuO nanoparticles and lower operating pressure were found to increase the heat transfer rate of heat pipe. Kumaresan et al. [22] indicated in their review, that the use of nanoparticles in the conventional fluid diminished the heat pipe dry out problems and increased its heat transport capacity. They also reported that the heat pipe orientation plays an effective role on its performance.

Based on the literature review, it is concluded that the suspension of nanoparticles in base fluid improves the thermal performance of heat pipes. There are many references available in heat pipes with mesh and sintered wicks, but none of them compared the thermal performance using these two wicks at fixed geometric and operating conditions. The effect of tilt angle on the performance of heat pipe using nanofluid is not much reported. This study effectively compares the performance of heat pipes viz. surface temperature distribution, thermal resistance and thermal conductivity using sintered and mesh wick structure, varying the working fluid, inclination angle and heat input.

2. Nanofluid preparation and its thermophysical properties

The surfactant free CuO/DI water nanofluid is prepared using a two-step method. Commercial CuO nanoparticles supplied by Alfa Aesar, USA is used in this study. The particles are spherical in shape and the maximum size is within 50 nm. The prepared solution is kept in an ultrasonicator for a duration of 1 h with 45 kHz frequency for better stability. Fig. 1(a) depicts the particle size distributions of CuO nanoparticles dispersed in DI water. The size of CuO nanoparticles has already been measured by the present authors and reported [19] using X-ray diffraction analysis. The Scherrer's formula is used to find the particle size and the result showed that the size of the particles does not exceed 39.1 nm. Further, a stability test has also been conducted for the mass concentration of 1.0% by keeping the prepared nanofluid statically for 60 days. After 60 days, a dynamic light scattering analysis (Zetasizer Nano ZS-Malvern) was conducted and from the results, the size of the nanoparticles was found to be around 250 nm. The increased size of the nanoparticles may be due to the slight agglomeration during the stability period. The prepared sample is kept for 60 days and no separation line was found between the nanoparticles and water. However, to ensure the stability of nanofluid, a Zeta potential test is conducted by Zetasizer and is shown in Fig. 1(b). The value for the given sample is +31.4 mV (a value above ±30 mV is believed to have good electrostatic stability), which confirms that the quality of the prepared sample is good and stable.

The thermophysical properties of the working fluid can be improved by the dispersion of CuO nanoparticles in the base fluid, mainly due to the enhancement in the thermal conductivity. Also, the addition of CuO nanoparticles increases the viscosity of working fluid and higher viscosity creates more restriction to the fluid flow. Hence, the thermal conductivity and viscosity of working fluid are experimentally measured. The thermal conductivity of CuO/DI water with different mass concentrations, viz. 0.5, 1.0 and 1.5 wt.% are measured by a KD2 Pro thermal properties analyzer (Decagon Devices, Inc., USA). The increases in the value of thermal conductivity for 0.5, 1.0 and 1.5 wt.% of CuO nanofluids are 0.96, 2.37 and 5.08% respectively. A Brookfield viscometer is used to measure the dynamic viscosity of nanofluid and it increases with mass concentration of CuO nanoparticles. The increases in viscosity for 0.5, 1.0 and 1.5 wt.% of CuO nanofluids are 8.91, 11.67 and 16.46% respectively. Rise in temperature of the working medium gradually reduces the viscosity and a maximum reduction of 54.93% is found for 1.5 wt.% of CuO/DI water nanofluid at 80 °C compared with 33 °C.

3. Heat pipe test rig and experimentation

The heat pipe used in this study has a length of 330 mm, an outer diameter of 12 mm and a thickness of 1 mm with copper as the pipe

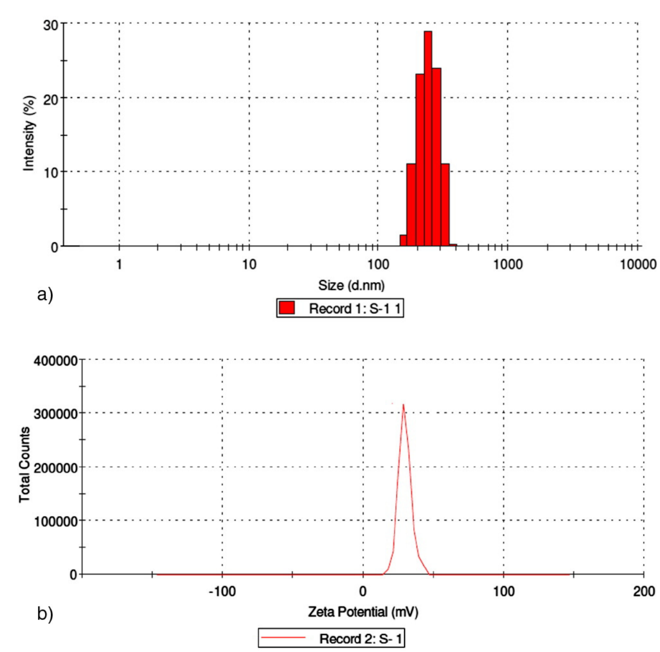

Fig. 1. (a) Particle size distribution and (b) Zeta potential analysis of CuO/DI water nanofluid.

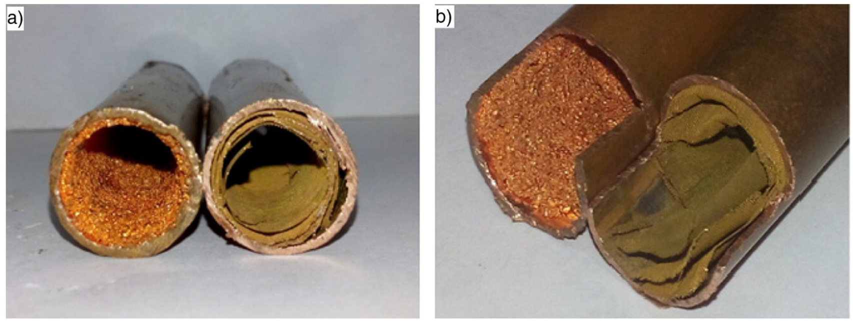

Fig. 2. Cross-sectional view of sintered and mesh wick heat pipes captured by digital camera (a) Front view and (b) Side view.

material. Totally eight heat pipes are used in this work, four heat pipes are made with sintered wicks and the remaining four with mesh wicks. In both the cases, one heat pipe is filled with DI water and the other three with CuO nanofluids. The wick thicknesses of both the heat pipes are maintained at a constant value of 1 mm. The screen mesh wicks are scrolled into cylindrical shape and tightly affixed with the inner surface of heat pipe, a thin stainless steel spring is inserted with a wire diameter and pitch of 300 μm and 10 mm respectively. Fig. 2 represents the detailed cross-sectional view of both sintered and mesh wick heat pipes. Five T-type thermocouples are attached over the surface of heat pipe, two at the evaporator section, one at the adiabatic section and the remaining two at the condenser section. The condenser section is cooled by liquid water to extract more amount of heat from the heat pipe compared with air cooling. The operating pressure and the quantity of working fluid filled in both sintered and mesh wick heat pipes are kept constant as 13.45 kPa and 7.3 ml respectively. Heat dissipation to the surrounding is minimized by insulating the test section using glass wool.

Experiments are conducted with MWHP and SWHP using DI water and three different concentrations viz. 0.5, 1.0 and 1.5 wt.% of CuO/DI water nanofluids. Fig. 3a & b shows the digital image of heat pipe test section experimental setup. The setup consists of an auto transformer, Caddo digital multimeter, variable angle holder, temperature control unit, Eureka Loflo meter (MG.9) and a data logger (Agilent) connected to a personal computer. Approximately 45 min duration is maintained between each heat input increment. The heat input starts from 10 W with an increment of 10 W till the heat pipe reaches dry out (SWHP with 1 wt.% CuO/DI water nanofluid reaches dry out at a maximum of 160 W). The heat pipe inclination angle is varied using a variable angle holder from its horizontal axis to 30, 45, 60, 75 and 90°.

4. Results and discussions

Experiments are conducted with sintered wick and mesh wick heat pipes till dry out conditions are attained. Steady state conditions are maintained throughout the study. For both the cases, heat input

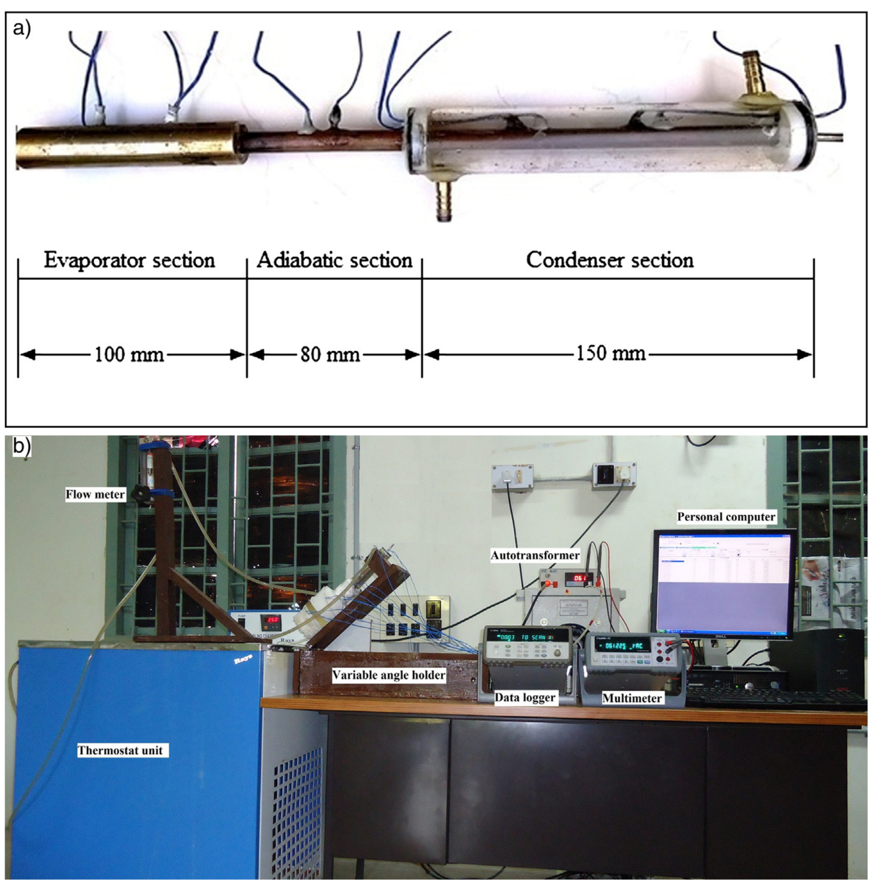

Fig. 3. (a) Layout of heat pipe test section and (b) Experimental setup.

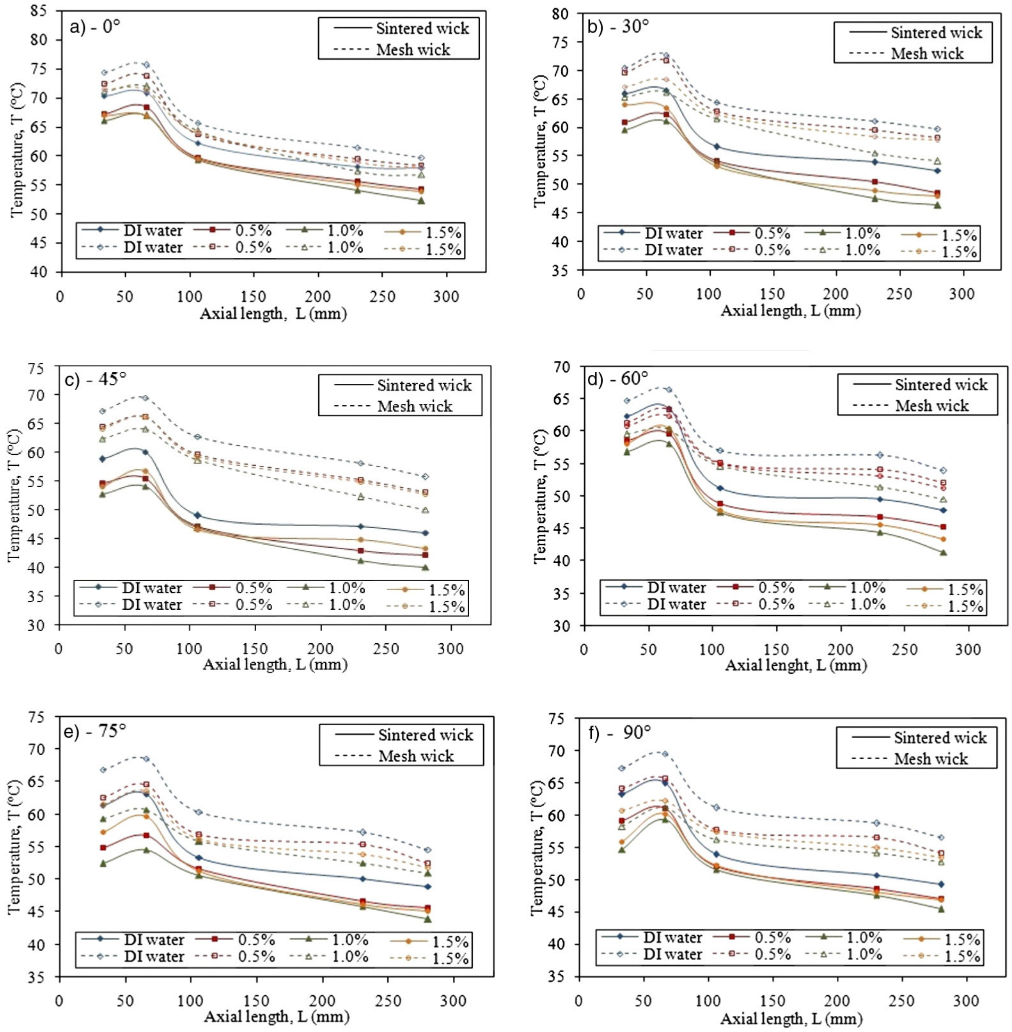

Fig. 4. (a–f) Surface temperature distribution in SWHP and MWHP for different concentrations of CuO/DI water nanofluids and inclination angles (Heat input — 100 W).

(10–160 W), kind of working fluid (DI water and CuO/DI water nanofluids) and tilt angle (0, 30, 45, 60, 75 and 90°) are varied and the effect of these parameters on the surface temperature distribution, thermal resistance and effective thermal conductivity is compared and analyzed. The enhancement for MWHP using CuO nanoparticles is from 100 to 120 W for horizontal position and it rises up to 140 W when the heat pipe is tilted. Another interesting observation is that the use of sintered wicks reduces the surface temperature and thermal resistance and improves the heat transport capacity compared with mesh wick. The heat transport capacity reaches a maximum of 160 W, when nanofluid is used and the heat pipe is tilted.

4.1. Surface temperature distribution

The surface temperature distribution in the SWHP and MWHP along the axial length is shown in Fig. 4(a–f). The results are plotted for 100 W heat input, because the MWHP with DI water reaches dry out condition at horizontal position after 100 W. Surface temperature distribution of the heat pipes has a strong influence on the heat transport capacity and the performance. In horizontal position with DI water as working fluid, the surface temperature of SWHP is lower than MWHP. Higher nucleate boiling heat flux is obtained in sintered wick heat pipe because of its higher porosity when compared with that of the mesh wick heat pipe (Fig. 7c). When CuO nanoparticles are dispersed in DI water, the surface temperature is significantly reduced throughout the heat pipe. It is clearly seen from all the graphs that the temperature distribution of both SWHP and MWHP using DI water is always higher than the CuO nanofluid heat pipes irrespective of the inclination angle. The reductions in temperatures of the evaporator section of SWHP at horizontal position are 3.1, 4.2 and 3.4 °C for 0.5, 1.0 and 1.5 wt.% of CuO/DI water nanofluid respectively compared with the base fluid, contrarily it is low i.e., 2.1, 3.4 and 2.9 °C for MWHP. This clearly shows that the CuO/DI water nanofluid reduces the surface temperature. The presence of high thermal conductivity nanoparticles in the working fluid improves its heat carrying capacity and enhances the boiling heat flux. In both the heat pipes, the maximum reduction in surface temperature is attained at 1.0 wt.% of CuO/DI water nanofluid and it decreases for mass concentration of CuO nanoparticles beyond this level (1.5 wt.%). Excess nanoparticles in the base fluid increase the fluid density, viscosity and thus create high flow resistance. It is concluded that a mass concentration of 1% produces better results and it is taken as optimum weight fraction.

Tilt angle has a strong influence on the surface temperature distribution of both SWHP and MWHP. The surface temperature gradually reduces with the increasing tilt angle. Interestingly the maximum reduction in temperature for both the heat pipes occurs at different orientations viz. 45° for sintered wick and 60° for mesh wicks. The variation in the temperature distribution is mainly due to the gravitational effect. The effect of gravity is more on sintered wick structure and it is observed that the copper sintered wick has good capillary action. For

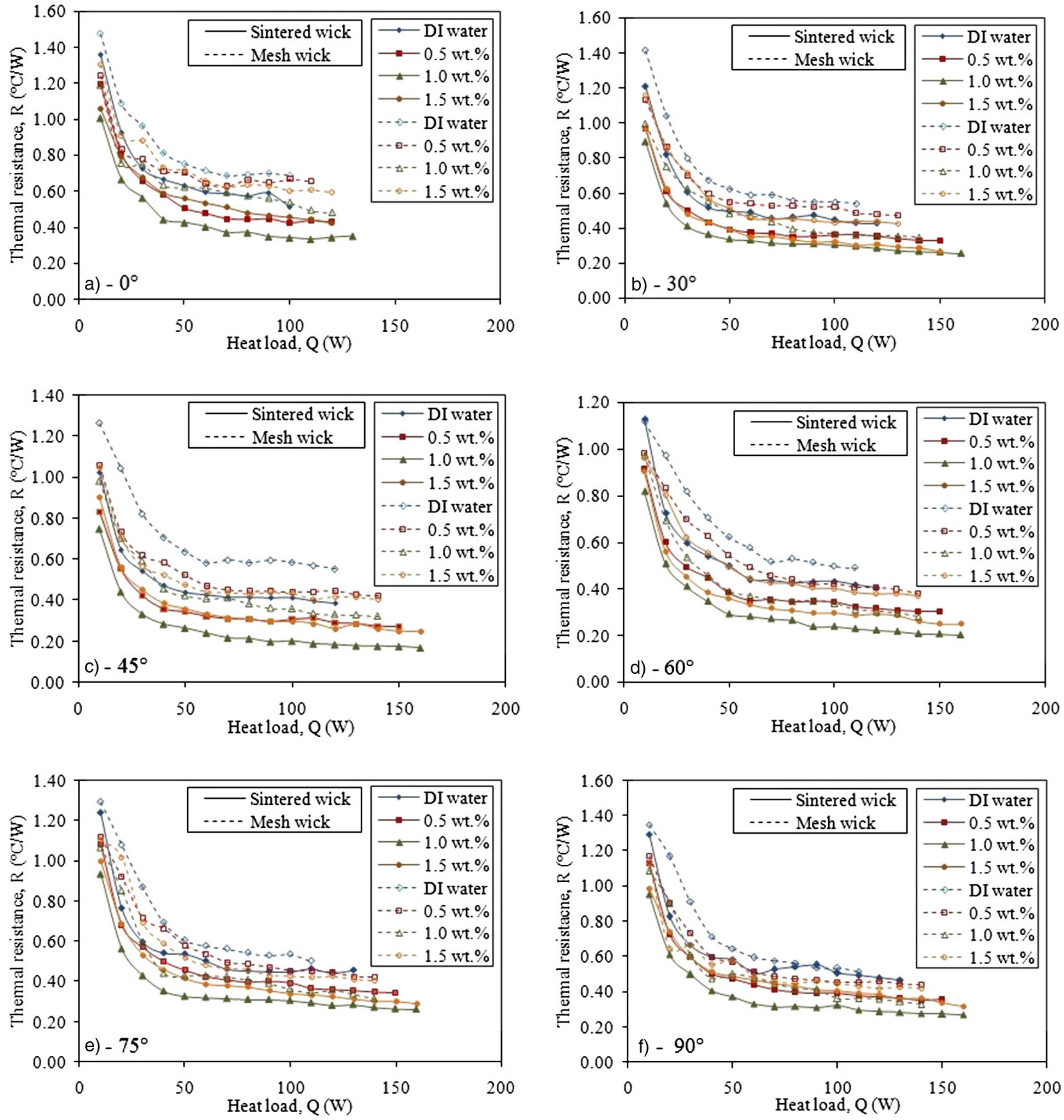

Fig. 5. (a–f) Thermal resistance variations of SWHP and MWHP for different concentrations of CuO/DI water nanofluids and inclination angles.

SWHP with 45° tilt angle the maximum reductions for 0.5, 1.0 and 1.5 wt.% of CuO/DI water nanofluids are respectively 4.2, 6.1 and 4.8 °C compared with DI water. Whereas for the same conditions, the temperature reductions obtained for MWHP are only 2.7, 4.8 and 3.1 °C. Even though the MWHP reaches its optimum performance at 60° tilt angle (3.4, 5.2 and 3.9 °C), its performance is still lower than the sintered wicks which are 3.8, 5.5 and 4.2 °C. It indicates that the SWHPs have better heat transport capacity than MWHP. Whenever the heat pipes are tilted beyond the optimum value or closer to the vertical position, the surface temperature distribution is increased. This is because, tilt angles beyond 45° for SWHP and 60° for MWHP induce quick return of working fluid to the evaporator which leads to the increase in temperature in the evaporator section.

4.2. Thermal resistance of heat pipes

Thermal resistance of a heat pipe is defined as the ratio of surface temperature difference between the evaporator and condenser sections and the heat input, where $Q = V \times I$. It is given by

$$R_{hp} = \frac{\overline{T}_{e,\,s} - \overline{T}_{c,\,s}}{Q} \tag{1}$$

Fig. 5(a–f) represents the thermal resistance vs heat input of SWHP and MWHP with DI water, varying mass concentrations of CuO/DI water and inclination angles. The graphs show that the thermal resistance of SWHP is lower than MWHP for all the cases. This is because the number of pores in the sintered wick surfaces is high and it encourages the nucleate boiling in the evaporator section compared with mesh wick surfaces. Thermal resistance has inverse proportionality with heat input and hence both SWHP and MWHP have high thermal resistance at low heat loads. This happens due to the formation of liquid layer in the evaporator section at low heat inputs and this layer disappears when the heat input is increased. All the figures show a rapid reduction in thermal resistance with heat input. When the heat load is increased from 10 W to 140 W, the reductions in thermal resistance achieved are respectively 76.58 and 67.22% for SWHP and MWHP for 1.0 wt.% of CuO/DI water at 45° tilt angle.

Addition of CuO nanoparticles with different weight fractions significantly reduces the thermal resistance for both types of heat pipes. During the boiling process, the addition of CuO nanoparticles deposited on the wick surface modifies the surface characteristics i.e., reduces the solid–liquid contact angle. Normally, the contact angle and surface wettability are having inverse proportionality [23]. Therefore, dispersion of CuO nanoparticles in the base fluid increases the surface wettability.

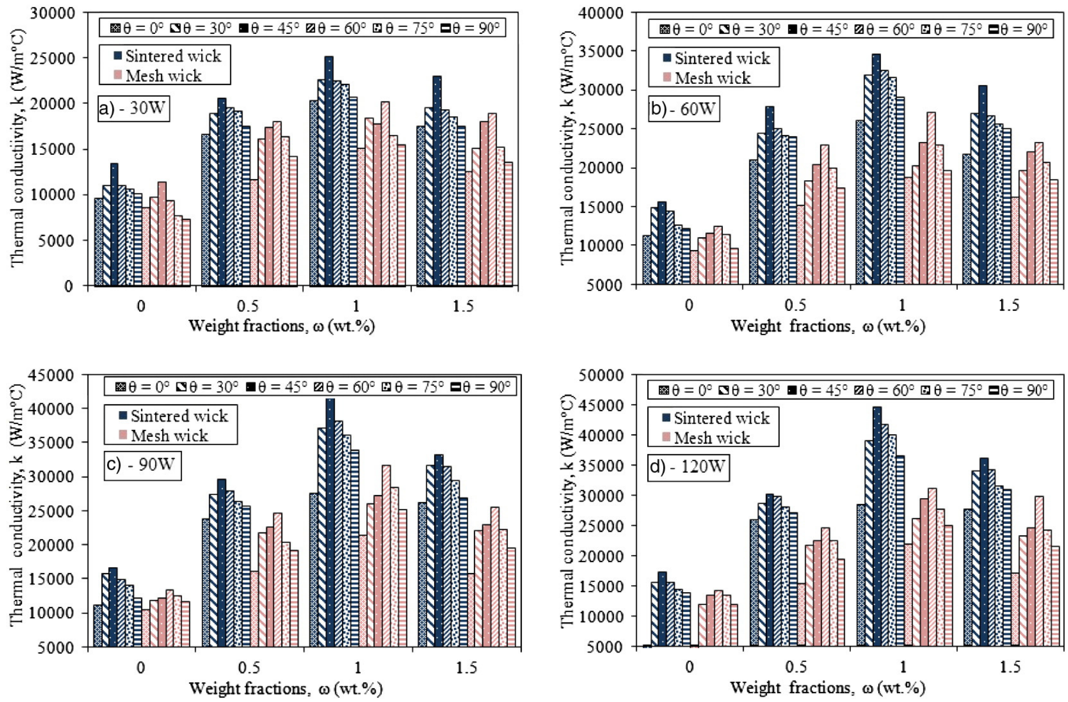

Fig. 6. (a–d) Effective thermal conductivity of SWHP and MWHP under varying weight fractions of CuO nanofluids, tilt angles and heat inputs.

Maximum reductions in thermal resistance observed at 45° tilt angle for 0.5, 1.0 and 1.5 wt.% of CuO/DI water SWHP are respectively 23.12, 49.64 & 31.37%, whereas for MWHP the values are 18.44, 35.44. & 21.23%. In both the heat pipes, the optimum weight fraction of nanofluid is found to be 1 wt.%. Inclination angle of heat pipes has a significant effect on the thermal resistance. Compared with the horizontal position, a remarkable reduction is observed with increasing tilt angle. It is gradually reduced and a maximum reduction is obtained at 45° for SWHP and 60° for MWHP. At 100 W heat input, 45° orientation is compared with 0° for SWHP and the results are 19.94, 27.75, 41.20 and 34.06% reduction using DI water, 0.5, 1.0 and 1.5 wt.% of CuO/DI water, the corresponding values for MWHP are 15.23, 21.98, 31.92 and 27.90% respectively. Even though 60° tilt angle and 1 wt.% are optimum for mesh wick, the reduction observed (36.86%) is less than that of sintered wick. Tilt angle beyond this optimum value results in higher thermal resistance. The reason for this deterioration is the same as that discussed in Section 4.1. From Fig. 5, it is observed that the dry out condition of the heat pipe is delayed by the dispersion of CuO nanoparticles and inclination angle. At 45° inclination and 1.0 wt.% of CuO nanofluid, the dry out occurs at 140 W and 160 W for mesh and sintered wick heat pipes respectively. This shows an improvement in the heat transport capacity of 14.28% for sintered wick compared with that of the mesh wick heat pipe.

4.3. Effective thermal conductivity

The effective thermal conductivity of a heat pipe depends on the heat input, surface temperature difference between the evaporator and condenser sections, length and cross-sectional area. It is given by the following equation,

$$k_{hp} = \frac{Q.L}{A_{c/s}\Delta T_s} \tag{2}$$

The variations in thermal conductivity of SWHP and MWHP with respect to different weight fractions of CuO/DI water nanofluids are shown in Fig. 6(a–d). The applied heat input varies from 10 to 160 W. To demonstrate in a simplified and an effective way, the results are picked out and plotted for 30, 60, 90 and 120 W only. The thermal conductivity gradually increases with heat input. Basically, heat supplied to the working fluid enhances its thermal conductivity and thus the heat pipe thermal conductivity. Moreover, CuO nanoparticles present in the base fluid also play a significant role in this enhancement. The maximum enhancements for SWHP at an optimized weight fraction of 1.0% and a tilt angle of 45° for 30, 60, 90 and 120 W heat inputs are respectively 19.39, 24.64, 29.97 and 36.50% compared with horizontal position. For the same conditions, MWHP gives the enhancements of 15.25, 19.57, 23.72 and 25.74% only. The maximum thermal conductivity achieved is about 44,601 W/m°C for SWHP with 1 wt.% of CuO nanofluid at 120 W heat input and 45° inclination angle. Whereas, the lowest thermal conductivity obtained is about 8475 W/m°C for MWHP with DI water at horizontal position. All the graphs show a higher thermal conductivity for SWHP than MWHP, because the sintered wick structure has strong capillary action compared with the mesh wicks.

Dispersion of CuO nanoparticles in the DI water tremendously increases the thermal conductivity of heat pipes and the maximum enhancement is observed for 1.0 wt.% of CuO/DI water combination. For SWHP with a heat input of 120 W and a tilt angle of 45°, the maximum enhancements achieved for DI water, 0.5, 1.0 and 1.5 wt.% of CuO/DI water nanofluids are respectively 21.59, 32.03, 42.86 and 36.48% compared with 30 W. For the same conditions, the enhancements observed for MWHP are only 14.56, 21.88, 33.18 and 26.45%. But the performance is deteriorated for 1.5 wt.% because the presence of more particles in the base fluid gives higher viscosity and thus increased flow resistance. Orientation of heat pipe also significantly enhances the thermal conductivity. The graphs indicate that the inclination of heat pipe gradually increases the thermal conductivity for both types. Optimum results are obtained at 45° for SWHP and 60° for MWHP which show that the impact of gravitational force in the mesh wick is higher than the sintered wick. However, SWHPs with inclination angles of 30, 45, 60, 75 and 90° are compared with the horizontal position for 120 W heat input and 1.0% mass concentration; it shows the enhancement in thermal conductivity for the above tilt angles are respectively 27.34, 36.50, 31.83, 29.17 and 22.35% and for MWHP these values are significantly lower.

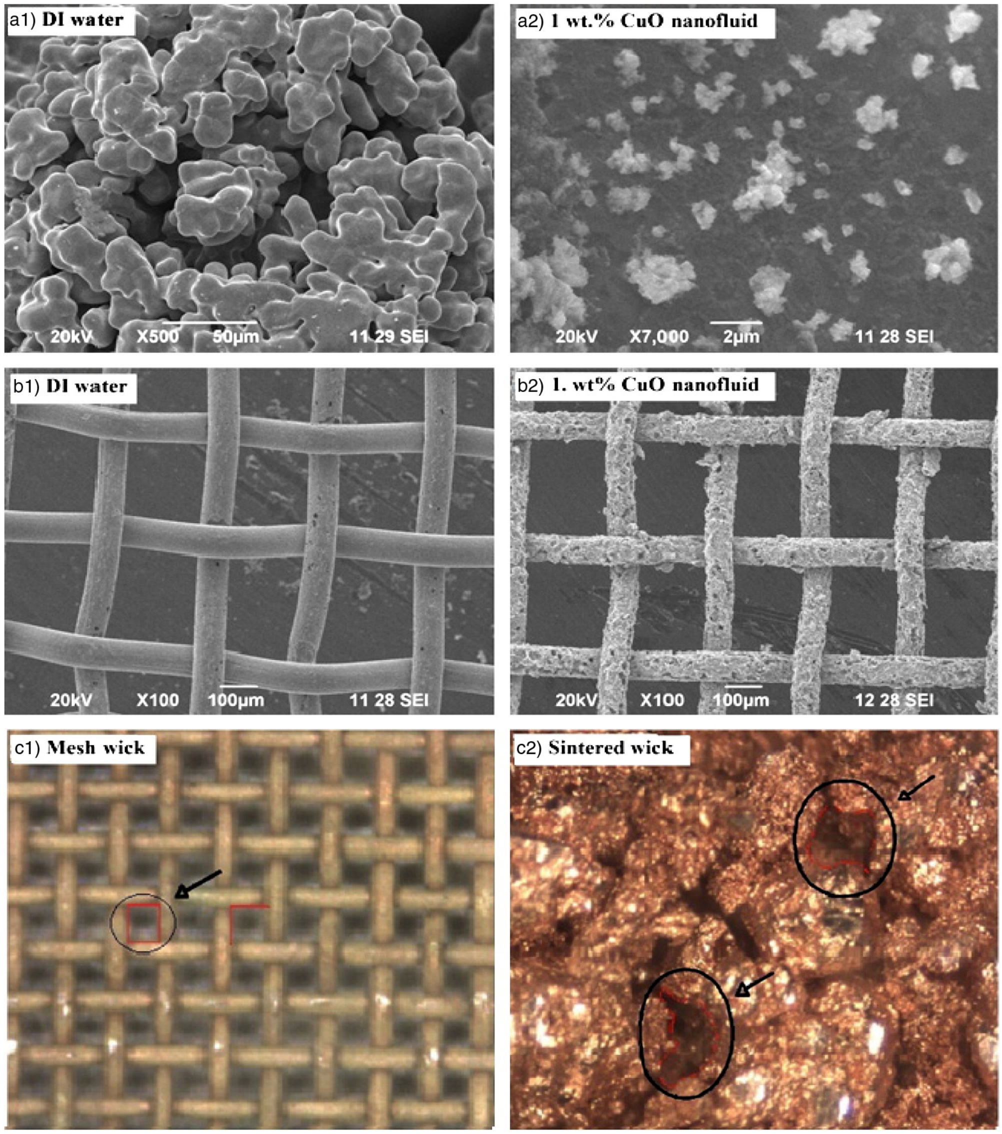

Fig. 7. Characterization of wick structures: SEM image of mesh and sintered wicks (a & b) and optical microscope image (c).

4.4. Analysis of wick structures

Fig. 7(a & b) represent the Scanning Electron Microscope (SEM) sintered and mesh wick structures with DI water and 1.0 wt.% of CuO/DI water nanofluid. Sintered wicks have better pore structure than mesh wicks as seen from the figures and they make easier for the liquid to flow from condenser end to evaporator. It is also seen from Fig. 7(a1) and (b1), that the heat pipes with DI water wick surfaces are clean and do not have any pore or particle deposition. However, the use of CuO nanoparticles leads to the formation of a thin porous coating layer over the sintered and mesh wicks. This layer increases the critical heat flux by improving the surface wettability and capillary force. Moreover, Fig. 7(b2) shows that the CuO nanoparticles coated over the sintered wick are evenly distributed than mesh wick and hence the function of CuO/DI water nanofluid in the sintered wick is more effective. Fig. 7(c) represents the pore size distribution of mesh and sintered wicks captured by an optical microscope. The pore size of the sintered wick is larger (0.10 and 0.11 mm^2) than the mesh wick (0.08 mm^2) and it permits more amount of liquid flow through the wick structures.

5. Conclusions

The heat transfer performance characteristics of sintered wick and mesh wick heat pipes are experimentally studied and compared using CuO/DI water nanofluids at various heat input and inclination angles. It is found that the heat transport capacity of sintered wick heat pipe is 14.3% more compared with mesh wick heat pipe under the same operating conditions. Similarly, a higher reduction in the surface temperature of 27.08% is observed for the sintered wick heat pipe with 1.0 wt.% of CuO/DI water nanofluids compared with mesh wick heat pipe. The inclination angle and weight percentage of CuO nanoparticles significantly influence the thermal performance of both the heat pipes. Optimum tilt angles of 45° and 60° respectively are observed for sintered wick and mesh wick heat pipes, whereas the optimum weight percentage is the same (1 wt.%) for both the cases. At these optimum conditions, a reduction in thermal resistance of 49.64% and 35.44% and an enhancement in the thermal conductivity of 36.50% and 29.84% are respectively observed for both sintered wick and mesh wick heat pipes. Based on the observed results, it is concluded that the thermal performance of sintered wick heat pipe is better than that of the mesh wick heat pipe.

References

[1] L. Lin, R. Ponnappan, J. Leland, High performance miniature heat pipe, Int. J. Heat Mass Transfer 45 (2002) 3131–3142.

[2] L.L. Vasiliev, Micro and miniature heat pipes—electronic component coolers, Appl. Therm. Eng. 28 (2008) 266–273.

[3] W. Chun, Y.H. Kang, H.Y. Kwak, Y.S. Lee, An experimental study of the utilization of heat pipes for solar water heaters, Appl. Therm. Eng. 19 (1999) 807–817.

[4] J.W. Wan, J.L. Zhang, W.M. Zhang, The effect of heat-pipe air-handling coil on energy consumption in central air-conditioning system, Energy Build. 39 (2007) 1035–1040.

[5] Y.H. Yau, Application of a heat pipe heat exchanger to dehumidification enhancement in a HVAC system for tropical climates—A baseline performance characteristics study, Int. J. Therm. Sci. 46 (2) (2007) 164–171.

[6] S.W. Kang, W.C. Wei, S.H. Tsai, S.Y. Yang, Experimental investigation of silver nanofluid on heat pipe thermal performance, Appl. Therm. Eng. 26 (2006) 2377–2382.

[7] G.-S. Wang, B. Song, Z.-H. Liu, Operation characteristics of cylindrical miniature grooved heat pipe using aqueous CuO nanofluids, Exp. Thermal Fluid Sci. 34 (2010) 1415–1421.

[8] K.H. Do, H.J. Ha, S.P. Jang, Thermal resistance of screen mesh wick heat pipes using the water-based Al_2O_3 nanofluids, Int. J. Heat Mass Transfer 53 (2010) 5888–5894.

[9] R. Saleh, N. Putra, S.P. Prakoso, W.N. Septiadi, Experimental investigation of thermal conductivity and heat pipe thermal performance of ZnO nanofluids, Int. J. Therm. Sci. 63 (2013) 125–132.

[10] M.K. Moraveji, S. Razvarz, Experimental investigation of aluminum oxide nanofluid on heat pipe thermal performance, Int. Commun. Heat Mass Transfer 39 (2012) 1444–1448.

[11] L.G. Asirvatham, R. Nimmagadda, S. Wongwises, Heat transfer performance of screen mesh wick heat pipes using silver–water nanofluid, Int. J. Heat Mass Transfer 60 (2013) 201–209.

[12] Y.H. Hung, T.P. Teng, B.G. Lin, Evaluation of the thermal performance of a heat pipe using alumina nanofluids, Exp. Thermal Fluid Sci. 44 (2013) 504–511.

[13] A.M. Hussein, K.V. Sharma, R.A. Bakar, K. Kadirgama, A review of forced convection heat transfer enhancement and hydrodynamic characteristics of a nanofluid, Renew. Sust. Energ. Rev. 29 (2014) 734–743.

[14] M. Bahiraei, A comprehensive review on different numerical approaches for simulation in nanofluids: traditional and novel techniques, J. Disp. Sci. Technol. 35 (2014) 984–996.

[15] C.K. Loh, E. Harris, D.J. Chou, Comparative study of heat pipes performance indifferent orientations, Annual IEES Semiconductor Thermal Measurement and Management Symposium, 2005, pp. 191–195.

[16] N. Putra, W.N. Septiadi, H. Rahman, R. Irwansyah, Thermal performance of screen mesh wick heat pipes with nanofluids, Exp. Thermal Fluid Sci. 40 (2012) 10–17.

[17] C.Y. Tsai, H.T. Chien, P.P. Ding, B. Chan, T.Y. Luh, P.H. Chen, Effect of structural character of gold nanoparticles in nanofluid on heat pipe thermal performance, Mater. Lett. 58 (2004) 1461–1465.

[18] R. Kempers, D. Ewing, C.Y. Ching, Effect of number of mesh layers and fluid loading on the performance of screen mesh wicked heat pipes, Appl. Therm. Eng. 26 (2006) 589–595.

[19] G. Kumaresan, S. Venkatachalapathy, L.G. Asirvatham, Experimental investigation on enhancement in thermal characteristics of sintered wick heat pipe using CuO nanofluids, Int. J. Heat Mass Transfer 72 (2014) 507–516.

[20] S. Kang, W. Wei, S. Tsai, C. Huang, Experimental investigation of nanofluids on sintered heat pipe thermal performance, Appl. Therm. Eng. 29 (5–6) (2009) 973–979.

[21] Z.H. Liu, Q.Z. Zhu, Application of aqueous nanofluids in a horizontal mesh heat pipe, Energy Convers. Manag. 52 (2011) 292–300.

[22] G. Kumaresan, S. Venkatachalapathy, A review on heat transfer enhancement studies of heat pipes using nanofluids, Front. Heat Pipes 3 (4) (2012) 1–8.

[23] Y. Takata, S. Hidaka, J.M. Cao, T. Nakamura, H. Yamamoto, M. Masuda, T. Ito, Effect of surface wettability on boiling and evaporation, Energy 30 (2005) 209–220.